[https://doi.org/10.21814/jus.5628]

Journal UMinho Science
Vol [03] | [2024]

[2975-951X]

RESEARCH ARTICLE

Cellular uptake, biodistribution and protection against oxidative damage by *Withania somnifera* leaf extract-loaded PCL and MPEG-PCL nanoparticles

G. MARSLIN[a], B. F. C. SARMENTO[b,c,d], J. F. R. FERNANDES[e], P. F. F. S. MOREIRA[e], O. M. F. P. COUTINHO[a], M. SÁRRIA PEREIRA DE PASSOS[f], A. C. GOMES[e]*, A. C. P. DIAS[e]*

Cite current issue: G. Marslin, B.F.C. Sarmento, J.F.R. Fernandes, P.F.F.S. Moreira, O.M.F.P. Coutinho, M. Sárria Pereira de Passos, A.C. Gomes and A.C.P. Dias, "Cellular uptake, biodistribution and protection against oxidative damage by *Withania somnifera* leaf extract-loaded PCL and MPEG-PCL nanoparticles", Journal UMinho Science, vol. [03], MM-2024, [https://doi.org/10.21814/jus.5628]

RECEIVED: 2024-02-06
ACCEPTED: 2024-02-19
PUBLISHED: 2024-10-18

ABSTRACT

Withania somnifera (WS) or Ashwagandha is a well-known medicinal plant, cultivated in dry areas of India and Pakistan, where it represents an important resource as a widely used medicinal crop. Because of its anti-inflammatory and immunomodulatory effects, its extract is used, alone or in combination with other herbal extracts, in the treatment of age-related and neurodegenerative disorders. For tapping on the important therapeutic potential of this resource for biomedicine, strategies for controlled delivery and biodistribution improvement are necessary to guarantee treatment efficacy. Pharmacological properties of WS leaf extract (WSE) are mainly attributed to the presence of withanolides. In the present study, WSE was encapsulated in nanoparticles composed of biodegradable polymers as poly-ε-caprolactone (PCL) and methoxy poly-ethylene

glycol poly-ε-caprolactone (MPEG-PCL) di-block copolymer. Laser doppler anemometry (LDA), X-Ray Diffraction (XRD) and Transmission Electron Microscopy (TEM) were used to analyze their size and shape. The particle size distribution of WSE-loaded PCL and MPEG-PCL nanoparticles was measured as 214-268 and 30-62 nm, respectively, presenting in both cases a spherical shape. U251 glioma cells, representative of the most common and lethal type of intracranial tumor which is glioblastoma, were exposed to these nanoparticles, demonstrating their efficient uptake. It was showed that MPEG-PCL nanoparticles containing WSE offered better protection to U251 cells against tert-butyl hydroperoxide (tBHP)-induced oxidative damage (95.1%), compared to PCL nanoparticles with WSE (56.4%) and free WSE (39.0%). In vivo distribution of these nanoparticles was further analyzed using zebrafish embryos to validate their biocompatibility in a relevant vertebrate neurodevelopment model.

KEYWORDS: *Withania somnifera*, PEGylated nanoparticles, neuroprotection, cellular uptake, zebrafish embryos.

1· INTRODUCTION

In recent years, herbal medicines have gained great attention due to the vast resource they represent of combined therapeutic efficacy and overall low toxicity, even at higher doses [1, 2]. *Withania somnifera* (WS) or Ashwagandha is a well-known medicinal plant distributed throughout India and Pakistan, used in Ayurveda and folk medicine since ancient times [3]. Owing to its medicinal notability and absence of significant associated side effects, the demand for this plant is high, leading to its cultivation in several areas, representing an important local resource for the producing countries as it is widely used as medicinal plant worldwide. In fact, as a reference, overall sales of WS products in the United States exceeded US$31 million in 2020 [4].

WS has been applied to treat several neurological ailments, geriatric fragilities, arthritis, behaviour-related disorders and stress [5]. Presently, numerous formulations (e.g. infusions, ointment powder and syrup, decoction) derived from various parts (leaves, fruits, roots) of WS have been utilized worldwide as therapeutics. Particularly interesting is the attention that the WS raw plant material and its originated extracts received at the US, being sold as supplements of diets to augment vitality and strength, immunity, and help the organism to overcome homeostasis disruption that may lead to disease [6]. A vast number of studies have investigated the pharmacological value of withanolides, the natural steroidal lactones found in WS. Because of its industrial relevance, metabolic engineering strategies and *in vitro* culture techniques have been employed to improve withanolide content compatible with commercial exploitation [6]. However, clinical application of WS extract (WSE) is restricted owing to low solubility in aqueous solvents, which reduces its bioavailability and *in vivo* pharmacokinetics, compromising its efficiency [7].

Water solubility is a characteristic of utmost importance for the development of a drug. A considerable percentage of novel pharmacologic entities failed to be effective due to their hydrophobicity [8]. It is therefore urgent to pursue advanced formulations with capacity to enhance

bioavailability of their content in a controlled manner, to enhance the plants bioactive compounds therapeutic use. Among these, nanocarrier-based drug delivery systems have demonstrated great success [9]. Indeed, a vast and diverse list of nanoparticles-mediated systems (*e.g.* liposomes, nanoemulsions, nanocapsules, phytosomes) to carry herbal bioactives have been developed, showing increased transport and release efficacy [10]. Incorporation of phyto-derived extracts into these nanostructured systems has the great benefit of overcoming foremost drawbacks, including their bulk dosing and decreased absorption, which attracted the attention of major stockholders in the pharmaceutic industry.

Additionally, the encapsulation of a drug within a polymer matrix not only helps prevent its degradation but also tends to enhance drug solubility, facilitate targeted delivery to specific sites, and reduce the occurrence of toxic side effects [11].

Plant active compounds encapsulated in polymeric nanoparticles demonstrated increased bioavailability and retention period of herbal therapeutics [10]. The incorporation of curcumin in this type of nanovesicles compose a good example, as its neuroprotective effect significantly increased, as compared to the free compound [12]. Similarly, quercetin which has great potential to treat Alzheimer´s disease was demonstrated to be effectively delivery to the brain via a polymeric type of nanosystems [13]. Another successful example is the nanoencapsulation of curcumin into methoxy poly(ethylene glycol) poly (ε-caprolactone) (MPEG-PCL), which lead to an increased cellular uptake and neuroprotective effect in glioma cells [14].

The delivery of drugs into brain is conditioned to their ability to efficiently transpose the blood brain barrier (BBB). Due to its protective function, the BBB tends to exclude the vast majority of brain-targeted drugs, an important consideration in the development of novel nanosolutions for drug delivery. Advantages and shortcomings of nanoparticle-mediated drug delivery to the brain have been reviewed [15, 16]. A particular aspect that has been much debated is the strong constriction that the endothelial cells of the BBB exert on molecules larger than 400,000 Da, so it is also reasonable to expect a lesser degree of obstruction for particles of nanometre size (<200 nm). However, nanoparticles uptake mechanisms are certainly different from drugs capable of entering the central nervous system (CNS), and it is unlikely that the nanoparticles cross the BBB and deliver drugs into brain without specific targeting properties. It was previously demonstrated that nanoparticles are capable of transposing the brain vasculature through the capillary endothelia, via cellular receptor or adsorptive-regulated endocytosis. Subsequently, their transcytosis to the basal side occurs so that these get into the brain parenchyma [17]. Surface functionalization of nanoparticles with ligands permit to overcome specificity limitations and contribute to ensure an efficient delivery across the BBB [17]. Another strategy being explored to deliver drugs directly to the brain is nose-to-brain delivery, which is also compatible with the physicochemical properties of polymeric nanoparticles [17].

MPEG-PCL is a block copolymer exhibiting a distinct amphiphilic structure that permits it to self-assemble into nanosize core shell spheres presenting hydrophobic segments as the inner core, and

hydrophilic ones as the outer shell [18]. A ready entrapment of lipophilic drugs can thus occur at the hydrophobic core, enabling their sustained release. On the other hand, the outer shell composed by the hydrophilic segment is particularly adequate to "camouflage" nanoparticles once administered intravenously, contributing to their effective escape from the reticuloendothelial system scavenging activity, thus leading to enhanced blood circulation times [18].

In the present study, leaf WSE-loaded poly (ε-caprolactone) PCL and MPEG-PCL nanoparticles were developed, and their cell uptake and protective activity against oxidative stress were evaluated *in vitro* using U251 human glioblastoma cells, representative of the most common and lethal type of intracranial tumor which is glioblastoma. In addition, *in vivo* biodistribution of these nanoparticles was analyzed using zebrafish embryos as vertebrate model.

2· MATERIALS AND METHODS

2.1· Plant material, cell line and chemicals

Aerial WS plant material was collected from the field (Bangalore, India), lyophilized under dark, powdered and stored in an airtight container. Standard withanolides (withanolide-A, withanolide-B, withanone, withaferin-A, 12-deoxy-withastramonolide) were a gift of Natural Remedies PVT Ltd., Bangalore India. Human glioblastoma-astrocytoma epithelial-like cell line (U251) was provided by the Faculty of Pharmacy, University of Porto (Porto, Portugal).

Coumarin-6, MTT (methylthiazolyldiphenyl-tetrazolium bromide) assay and stannous octoate ($Sn(Oct)_2$ were acquired from Sigma-Aldrich (Barcelona, Spain). Poly(ethylene glycol) methyl ether (MPEG, Mn 2000, Fluka, USA), ε-caprolactone (ε-CL, Alfa Aesar, USA), and the cell culture components, namely Dulbecco's Modified Eagles Medium (DMEM, high glucose content, Sigma, Spain) and fetal bovine serum (FBS), were purchased to BioChrom KG (Berlin, Germany). All solvents used were of HPLC (High-Performance Liquid Chromatography) high analytical grade, obtained from Merck (Darmstadt, Germany). Synthesis and characterization of block copolymer MPEG-PCL was according as described elsewhere [14].

2.2· Preparation of *Withania somnifera* leaf extract (WSE)

Leaves of *Withania somnifera* (WS) were used for the WSE preparation. Briefly, 50 g of finely powdered WS leaves were extracted in aqueous methanol (90%, V/V) by sonication for 1 h, in a water bath at 25º Celsius, in the dark. The resulting solution was filtered with a 0.45 μm nylon membrane (Poll Corporation, USA), and purified with dichloromethane. The solvent was then removed on a Rotavapor R-300 (Buchi, Switzerland) at 40 ºC, while the remaining residue was lyophilized to acquire a gummy powder (WSE).

A Merck-Hitachi LaChrom Elite HPLC apparatus (Hitachi, Japan) coupled to a Diode-Array Detector (DAD), and using a Purospher RP-18 5 μm (Merck, Germany), was run on WSE to validate the presence of bioactive compounds. To the elution protocol, it was used 0.1% (V/V) of

acetic acid-water (eluent A) and 0.1% (V/V) of acetic acid-acetonitrile (eluent B), following a linear gradient starting at 45% (V/V) A to 90% (V/V) A, for 35 min. DAD results were collected and the data detected for all peaks were accumulating in the range of 200-400 nm, while chromatograms were recorded at 235 nm. Quantification was performed by the external method recurring to pure standards (Natural Remedies, Bangalore, India).

2.3· Preparation of WSE encapsulated nanoparticles

WSE nanoformulations were prepared via solvent displacement method, as described by Marslin et al (2014) [14]. Among the different amounts of WSE tested (5, 10, 15 and 20 mg), 10 mg of WSE demonstrated particularly higher loading efficiency (data not shown). As so, 10 mg of WSE and 100 mg of PCL or MPEG-PCL were dissolved in 5 mL of dichloromethane (DCM), which was subsequently dropped into 50 mL of an aqueous solution containing 1% (V/V) of Pluronic (F-68), and maintained under stirring for 4 h. Finally, residual organic solvents were removed under reduced pressure at 37°C using Rotavapor R-300 (Buchi, Switzerland). The obtained suspension was then centrifuged at 45,000 g for 15 min, to pellet down the nanoparticles. The resulting pellet was freeze-dried and stored at 4°C for future use. PCL and MPEG-PCL nanoparticles were first prepared in the absence of WSE. To investigate for the best features, different WSE-containing nanoparticles were prepared by altering the polymer and stabilizer proportions (Table 1).

For in vitro cellular uptake and *in vivo* biodistribution studies, coumarin-6 was co-encapsulated with WSE (WSE-C) into the nanoparticles, following the aforementioned protocol. A slight adjustment was performed by dissolving coumarin-6 (2 mg) and WSE (8 mg) in 5 mL of DCM.

2.4· Physicochemical characterization of WSE loaded nanoparticles

2.4.1· Particle size, polydispersity index and zeta potential

Particle size, polydispersity index (PdI) and zeta potential of the nanoparticles were measured using a Zetasizer (Zetasizer nano ZS, Malvern Instruments, UK). A volume of 500 µL of a sample was diluted in 500 µL of double-distilled water, and a zeta dip cell was used to assess the zeta potential, which was determined based on the electrophoretic mobility of the nanoparticles in an aqueous solvent, recurring to laser Doppler velocimetry and phase analysis light scattering.

Table 1 – Polymer, extract and Pluronic (F-68) composition used to prepare various batches of nanoparticles. WSEP: WSE-loaded PCL nanoparticles; WSEM:WSE-loaded MPEG-PCL nanoparticles. (*) Highlighted formulations correspond to those used at the subsequent studies.

Formulation code	WSE (mg)	Polymer (mg)	Organic solvent (mL)	Pluronic (w/v %)
WSEP 1	10	50	5	0.5
WSEP 2	10	100	5	0.5

WSEP 3	10	50	5	1
WSEP 4 *	10	100	5	1
WSEP 5	10	100	5	1.5
WSEM 1	10	50	5	0.5
WSEM 2	10	100	5	0.5
WSEM 3	10	50	5	1
WSEM 4 *	10	100	5	1
WSEM 5	10	100	5	1.5

2.4.2. Nanoparticles morphology

Morphology of the nanoparticles was analysed by Transmission Electron Microscopy (TEM, JEOL-1400, 902A Jeol Ltd) analysis. In brief, 50 µL of freshly prepared WSE loaded nanoparticle suspension was dropped onto a copper grid (400 mesh), and allowed to air dry. Dried samples were then negatively stained with 2% (w/w) sodium phosphotungstate, and the images were recorded.

2.4.3. X-ray diffraction analysis

XRD studies were conducted using an X-ray diffractometer (Philips, PW1710) coupled to a horizontal goniometer. Samples were placed in the proper holder and scanned at a rate of 1° min^{-1} from 0° to 60°.

2.4.4. Differential scanning calorimetry (DSC)

The physical state of WSE entrapped at the nanoparticles was studied by DSC (Universal V4.7A TA Instruments). Data on the endothermic melting temperature of the leaf extract, polymers and nanoparticles were collected by placing 5-10 mg samples on aluminum pans with the lids, and scanned between 25°C and 200°C, at the rate of 5°C per min, under a nitrogen atmosphere.

2.4.5. Encapsulation efficiency

Concentration of withanolides encapsulated in the nanoparticles was determined by HPLC. For this, 20 mg of WSE loaded nanoparticles was dissolved in 2 mL of methanol, and sonicated for 5 min to guarantee their disruption. Samples were then centrifuged at 25,000 g for 10 min to obtain a clear supernatant for analysis. HPLC studies were performed as described.

The encapsulation efficiency was calculated as follows:

$$\text{Encapsulation efficiency} = \frac{Amount\ of\ extract\ or\ withanolides\ in\ the\ nanoparticles}{Total\ amount\ used\ for\ preparation} \times 100$$

2.4.6. In vitro release profile

In vitro release studies were carried out using a dialysis bag with a molecular weight cut-off of 12,000-14,000 Da. Prior to its use, the semi-permeable membrane was kept in phosphate buffered saline (PBS) at pH 7.40 for 12 h. Next, 20 mg of WSE loaded nanoparticles were added to the dialysis bag. The dialysis tubes were incubated in 50 mL of pre-warmed PBS (37°C, pH 7.40) and 1% (v/v) Tween 80. To investigate the release profile of withanolides from the nanoparticles, the liberation of the major compound withanolide-A was quantified via HPLC as described above. 1 mL samples were collected from the incubation medium after different intervals. Subsequently, an equal volume of fresh PBS at pH 7.40 was immediately added.

2.5· Cell culture

Human glioma U251 cells were cultured in Dulbecco's Modified Eagle Medium (DMEM; ref. D6429, Sigma-Aldrich, Spain) supplemented with 1% (V/V) streptomycin, 2 mM L-glutamine, 10% (V/V) FBS, and incubated in a 5% CO_2 incubator at 37°C.

2.6· Cell viability assessment

The MTT assay provides information about cell viability by measuring the proportion of metabolically active cells in a population. A decrease in MTT reduction indicates a decrease in cell viability due to cytotoxicity or other adverse effects.

The effect of WSE and WSE-loaded nanoparticles on cell metabolic activity was measured using MTT assay. In brief, U251 cells were plated onto 24-well flat-bottom plates (Orange Scientific products, Belgium) at a concentration of 2×104 cells/mL in DMEM. After incubation for 24 h at 37°C, the culture medium was removed and replaced by 500 µL of various test concentrations, diluted in fresh culture medium, of free and nano-encapsulated WSE. To ascertain the influence of the polymer on cell metabolic viability, empty nanoparticles were also tested as control. After 48 h of treatment with WSE, WSE-loaded and empty nanoparticles, the incubation medium was removed and again exchanged by 500 µL of fresh culture medium containing MTT (0.5 mg/mL in Krebs medium, pH 7.40). After 4 h, the MTT solution was discarded and 500 µL of solvent (containing 1:1 (V/V) of DMSO and ethanol) was added to the wells. Plates were shaken for 10 min at RT under dark, to solubilize the formazan crystals formed. Absorbance of the subsequent formazan solution was measured at 570 nm, using a microplate reader (Synergy™ H Multi-mode Microplate Reader, BioTek Instruments, USA). The amount of MTT that is converted to formazan at the cell microenvironment reflects their redox status (metabolic activity), and correlates with cell viability, which was also determined via the LDH leakage assay, as described in the literature [19].

2.7· Cellular uptake of nanoparticles

U251 cells were seeded in 24-well plates at a density of 2×10^4 cells/mL, and allowed to adhere and proliferate for 24 h. Cells were then co-incubated with 5 µg/mL PCL or MPEG-PCL nanoparticles-loaded with WSE-C. Following different periods of exposure (2, 4 and 24 h), cells were washed three

times with PBS pH 7.40 to eliminate any PCL or MPEG-PCL nanoparticles containing coumarin-6 that were not internalized. Then, cells were fixed in 4% (V/V) paraformaldehyde, and their nuclei was stained with Hoechst. At last, a photographic record was collected under a fluorescent microscope equipped with digital camera (Olympus 1X71).

2.8· Protection against cellular oxidative damage insult

To evaluate the cytotoxic effect of tert-butyl hydroperoxide (tBHP) in U251 cells, 0.1, 0.25, 0.5 and 1 mM of tBHP were tested for 1, 2 and 3 h. Then, the experimental conditions of tBHP that yield the most significant (circa 50%) cellular oxidative damage (in this case, 1 mM of tBHP for 3 h) was incubated together with different concentrations of WSE and WSE-loaded nanoparticles. The percentage of protection conferred against oxidative stress was calculated considering the following equation:

$$\% \text{ of Protection} = \% \text{ of Cell Viability}_{\text{Ext +ins}} - \% \text{ of Cell Viability}_{\text{ins}}$$

Whereas,

$\text{Cell Viability}_{\text{Ext +ins}}$ = % of cell viability with tBHP and WSE-loaded nanoparticles, relatively to the control cells

$\text{Cell Viability}_{\text{ins}}$ = % of cell viability with tBHP, relatively to the control

The oxidative output derived by tBHP in U251 cells, under the experimental conditions tested, was also investigated by quantification of lipid peroxidation levels, using the thiobarbituric acid reactive substance (TBARS) assay, as described elsewhere [18].

2.9· *In vivo* biodistribution of WSE-C nanoparticles in zebrafish embryos

The breeding protocol for zebrafish was performed according to a previous work [19]. Viable eggs at early blastula stage (approximately 2 hours post fertilization, h_{pf}) were separated from unviable ones (absence of transparency) using a stereomicroscope (Nikon Eclipse TS 100). Embryos were then washed twice with sterilized freshwater, and randomly allocated into 24-well microplates for continuous waterborne exposure with WSE, empty and WSE-loaded MPEG-PCL and PCL nanoparticles for 80 h_{pf}. Zebrafish embryos were derived from the same progeny of eggs, with a fertilization rate higher than 90%. Ten embryos were incubated in a final volume of 2 mL per well. Each condition was performed in quadruplicate. Incubation media was renewed daily, and embryos demonstrating absence of heart beating or coagulated were removed, to avoid cross contamination. Two nominal concentrations (0.25 and 1 μg/mL) were tested. To ensure optimal incubation temperature of the embryos, all samples were pre-heated at 28±1°C. Zebrafish embryogenesis was

followed until 80 h_{pf}, and recorded under a fluorescent microscope (Olympus IX71). This study was conducted following OECD standards [19], i.e. only zebrafish embryos up to 120 hpf were used, and therefore no statutory ethical approval was required [20].

2.10· Statistical analysis

All data were analyzed using GraphPad Prism version 5 for Windows, GraphPad Software, Boston, Massachusetts USA. At graphs, data are expressed as mean±standard deviation (SD) of the indicated number of independent experiments. The significance of differences between mean values was estimated using the unpaired two-tailed Student's *t*-test. A *P* value of 0.05 was considered for significance testing.

3· RESULTS

3.1· Characterization of WSE loaded nanoparticles

The composition of WSE was evaluated by HPLC-DAD, and the major compounds present identified and quantified (Figure 1). WSE showed to contain several withanolide type compounds, namely withaferin-A and withanolide-A. WSE compounds are poorly soluble in water due to their hydrophobicity. Although WSE was not soluble in water, its nanoformulations can be completely dispersed in water (Figure 2).

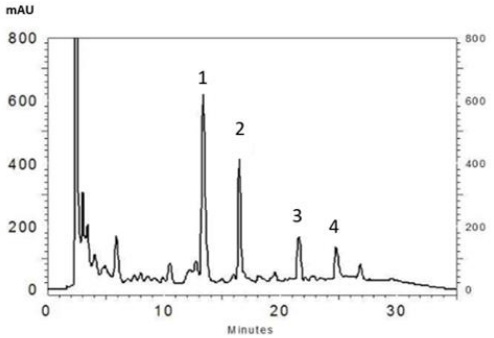

Compounds	mg/g dw extract
withaferin-A (1)	368
withanolide-A (2)	124
withanone (3)	70
12-deoxy-withastramonolide (4)	56

Figure 1 — *Withania somnifera* leaf extract (WSE) HPLC chromatogram recorded at 235 nm, and its composition (mg compound per g of dry weight extract). "mAu" stands for milli arbitrary units.

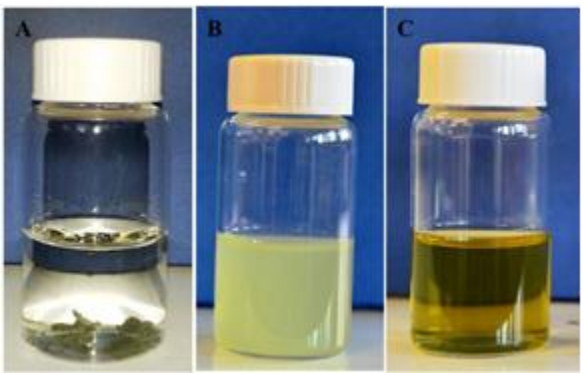

Figure 2 — A. Aqueous solubility of WSE B. WSE-loaded PCL nanoparticles C. WSE-loaded MPEG-PCL nanoparticles.

3.2· Particle size, polydispersity index and zeta potential

The amount of polymer and stabilizer used in the nanoformulations affected particle size (Table 2). The size of WSE-loaded PCL nanoparticles ranged from 214.25±2.30 to 268.32±3.20 nm, whereas the WSE-loaded MPEG-PCL nanoparticles were much smaller in size (30.76±1.29 to 62.32±3.70) (Table 2).

Table 2 – Characterization and encapsulation efficiency of WSE-loaded PCL and MPEG-PCL nanoparticles. Values are expressed as mean±standard deviation (SD) (n=3). WSEP: WSE-loaded PCL nanoparticles; WSEM: WSE-loaded MPEG-PCL nanoparticles.

Formulation code	Particle size (nm±SD)	Polydispersive index (PdI±SD)	Zeta potential (mV±SD)	Encapsulation efficiency (%±SD)
WSEP 1	242.12±3.24	0.31±0.02	-34.20±2.20	39.08±2.15
WSEP 2	268.32±3.60	0.36±0.20	-32.42±3.10	46.06±3.52
WSEP 3	240.28±4.20	0.28±0.14	-30.20±2.10	42.16±2.32
WSEP 4	214.25±2.30	0.24±0.26	-30.14±2.60	59.26±3.31
WSEP 5	224.27±2.30	0.20±0.06	-29.14±2.80	49.21±3.72
WSEM 1	43.40±2.70	0.30±0.12	-15.30±0.90	46.62±2.82
WSEM 2	62.32±3.70	0.38±0.15	-14.00±1.53	53.30±1.21
WSEM 3	31.24±0.80	0.33±0.01	-12.70±1.20	44.72±3.13
WSEM 4	30.76±1.29	0.36±0.04	-7.90±1.60	72.82±0.80
WSEM 5	42.70±2.26	0.32±0.05	-11.90±1.60	54.12±1.20

Size and PdI characterization of WSE-loaded PCL and MPEG-PCL nanoparticles by DLS are presented at Figure 4. The physicochemical properties of empty PCL and MPEG-PCL nanoparticles were previously reported [21]. Zeta potential of WSE loaded MPEG-PCL and PCL nanoparticles were -7.90±1.60 mV and -30.14±2.60 mV, respectively.

In the present study, an encapsulation efficiency between 44.72±3.13 to 72.82±0.80% was observed for MPEG-PCL nanoparticles (see Table 2). TEM imaging of the WSE-loaded PCL and MPEG-PCL nanoparticles revealed an almost spherical shape (Figure 3).

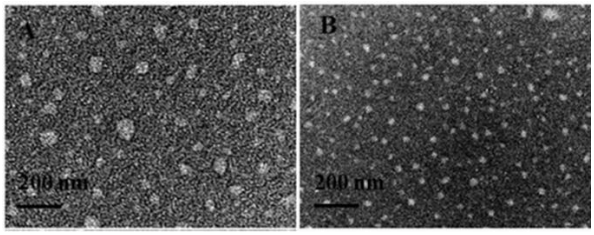

Figure 3 — Morphological characterization of WSE-loaded PCL and MPEG-PCL nanoparticles. **A.** TEM images of WSE-loaded PCL **B.** and of WSE-loaded MPEG-PCL nanoparticles.

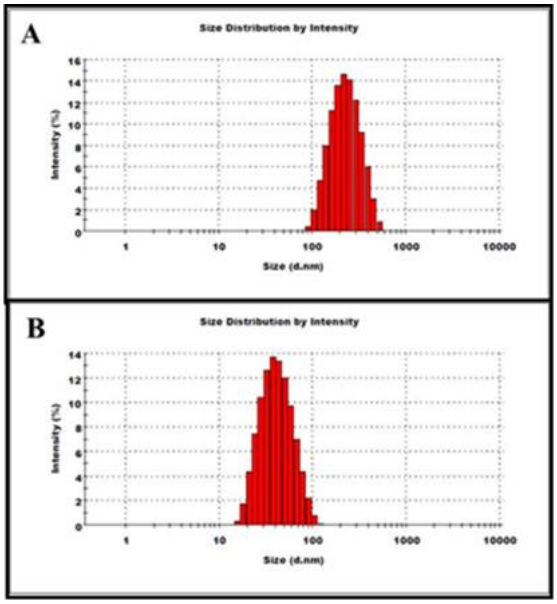

Figure 4 — **A.** Particle size distribution of WSE-loaded PCL nanoparticles **B.** and of WSE-loaded MPEG-PCL nanoparticles.

3.3· Differential scanning calorimetry (DSC) analysis

The DSC chromatogram of WSE showed a melting endothermic peak at 111.26°C (Figure 5). Yet, no melting peak was perceived for either PCL or MPEG-PCL nanoparticles, demonstrating the non-crystalline nature of the nano-encapsulated extract, at least considering the particle surface level. Hence, it could be inferred that at the nanoparticles, the WSE presented an amorphous or disordered crystalline nature of a molecular dispersion, or a solid solution state in the PCL/Pluronic F68 and MPEG-PCL/Pluronic F68 matrix, subsequently to fabrication.

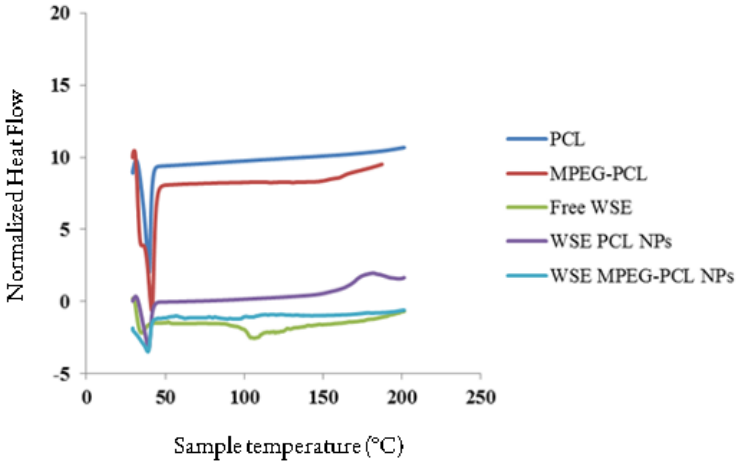

Figure 5 — Differential scanning calorimetric thermogram of polymers, WSE and WSE-loaded nanoparticles (NPs).

3.4· X-ray diffraction (XRD) analysis

The XRD data of MPEG-PCL, WSE, WSE-loaded PCL and MPEG-PCL nanoparticles are reported in Figure 6. The XRD results on WSE demonstrated diffraction peaks at 2θ value of 22.40, pointing to a crystalline nature. However, these characteristic peaks suggestive of crystallinity were not observed for WSE-loaded PCL and MPEG-PCL nanoparticles, indicating thus their amorphous state. On the other hand, the XRD outline of the physical mixture diffraction peaks of MPEG-PCL

and WSE showed a partial dissolution, and the occurrence of a crystalline state for WSE in the polymer.

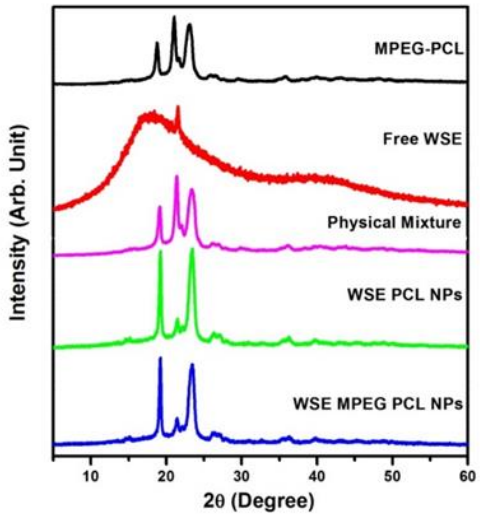

Figure 6 — X-Ray Diffraction patterns of MPEG-PCL, WSE and their physical mixture, and WSE-loaded PCL and MPEG-PCL nanoparticles (NPs). "Arb. Unit" stands for arbitrary units.

3.5· Extended release of WSE from the nanoparticles

The *in vitro* liberation profile of WSE from the nanoparticles was investigated in PBS pH 7.40, at 37°C. Since withaferin-A, withanolide-A, withanone and 12-deoxy-withastromonolide are major and key-pharmacological compounds of WSE, its release into the medium was quantified. Figure 7 shows the release kinetics of these compounds from the free WSE and the WSE-loaded PCL and MPEG–PCL nanoparticles for 7 days. Free WSE released much faster into the surrounding medium from the dialysis bag than WSE-loaded PCL and MPEG-PCL nanoparticles. A quick release (30-40%) of the drug from the WSE-loaded PCL and MPEG–PCL nanoparticles was observed for the first 6 h. It took another 162 h to reach a cumulative release of 80% from these nanoparticles.

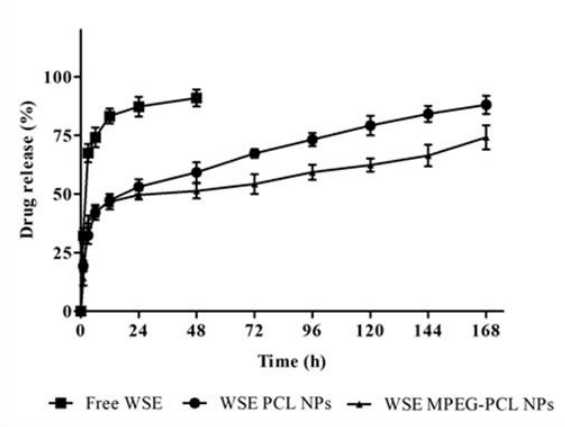

Figure 7 — Releasing profile of free WSE, WSE-loaded PCL and WSE-loaded MPEG-PCL nanoparticles (NPs) from the dialysis bag.

3.6. In vitro cytotoxicity of WSE and nanoparticles

Among different doses of WSE tested, nominal concentrations up to 10 μg/mL did not affect cell viability, in comparison to the control group (cells not exposed to WSE). WSE at 25 μg/mL (and above) had a negative effect when compared to the control group (Figure 8A). From these results, it is evident that high concentrations of WSE decreases cell viability. Likewise, 25 μg/mL of WSE-

loaded PCL and MPEG-PCL nanoparticles significantly affected cell viability, whereas lower concentrations (0.1, 1 and 10 µg/mL) did not (Figure 8B). Hence 0.1, 1 and 10 µg/mL of WSE-encapsulated PCL and MPEG-PCL nanoparticles were selected for subsequent assays.

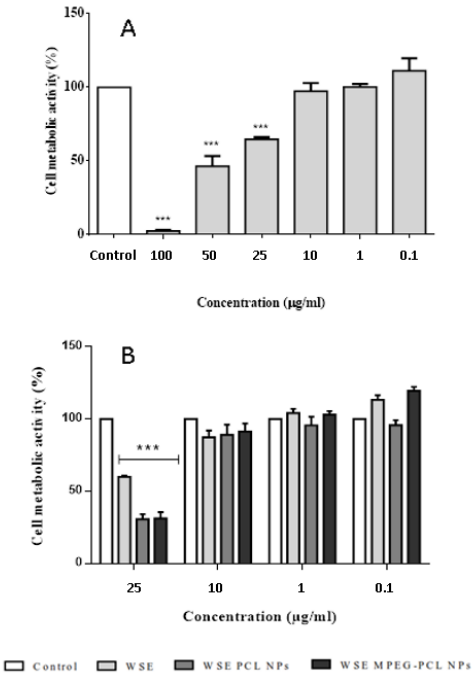

Figure 8 — Effect of free WSE (A) and of WSE-loaded PCL and MPEG-PCL nanoparticles (B) on metabolic activity of human glioma cells (U251, 2×10^4 cell/mL) measured by the MTT assay. Data presented (mean±SD, n=3). Statistical analysis was performed using one sample t-test. Asterisks (*) denotes statistically significant differences from control group (only cells) (***P<0.001).

3.7. Cellular uptake of WSE-loaded nanoparticles

Cellular uptake of WSE-loaded PCL and MPEG-PCL nanoparticles were studied using co-encapsulation of coumarin-6 (WSE-C), as reported [22]. As observed at Figure 9, cells exposed to WSE-C-loaded MPEG-PCL nanoparticles demonstrated considerable fluorescence intensity as compared to cells incubated with PCL nanoparticles at equivalent concentration (10 µg/mL), permitting to anticipate that the MPEG-PCL nanoparticles should have been uptaken more efficiently than PCL nanoparticles.

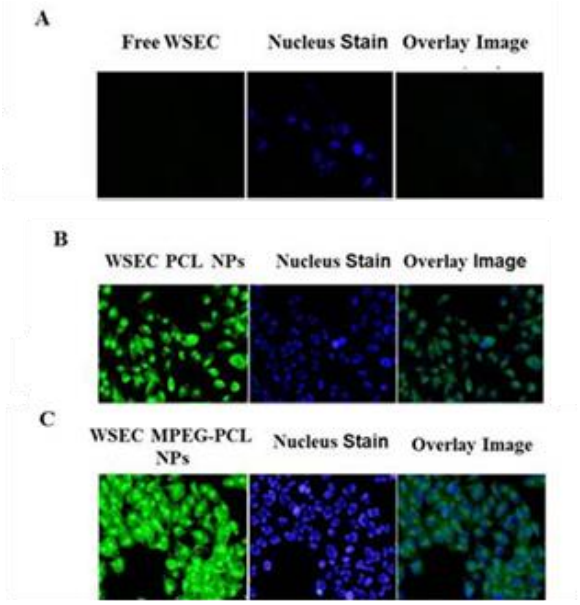

Figure 9 — Human glioblastoma cells (U251) incubated with WSE-C-loaded PCL and MPEG-PCL nanoparticles (NPs) for 2 h. NPs are visualized by incorporating coumarin-6 (green). After treatments, cells were analyzed for fluorescence intensity. Fluorescent images of free WSE-C (**A**), WSE-C-loaded PCL (**B**) and WSE-C-loaded MPEG-PCL nanoparticles (**C**) showing their internalization by human glioma cells.

3.8. WSE nanoparticles protects against oxidative stress-mediated cytotoxicity

tBHP is a ROS producing agent with capability to induce lipid peroxidation. It has been used as a model substance to induce oxidative damage to cells [23]. tBHP is also well recognized by its potential to decrease cell proliferative life span, and increase senescence-linked enzyme activities [24], leading thus to oxidative stress-induced premature senescence. To optimize the tBHP concentration that could trigger oxidative cell damage, a range of nominal concentrations (0.1, 0.25, 0.5 and 1 mM of tBHP) were analyzed at different incubation periods (Figure 10). Obtained results revealed that 1 mM tBHP induced significant viability loss (by 50%) to U251 cells after 3 h of incubation. Additionally, under these conditions' cells suffered significant lipid peroxidation induced by tBHP (data not shown). Hereafter, 1 mM tBHP for 3 h incubation were the experimental conditions selected for the subsequent experiments.

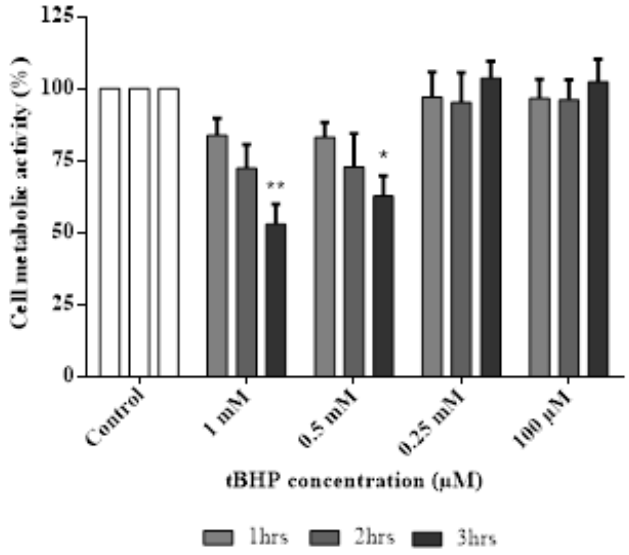

Figure 10 — Effect of tBHP concentration and time exposure on metabolic activity of U251 cells measured by MTT assay. Data presented (mean±SD, n=3). Statistical analysis was performed using one sample t-test. Asterisks (*) denotes statistically significant difference from control group (only cells) (*P<0.05;

Three different nominal test concentrations (0.1, 1 and 10 µg/mL) of free WSE, equivalent WSE-loaded PCL and MPEG-PCL nanoparticles, and both PCL and MPEG-PCL empty nanoparticles were evaluated for their ability to protect U251 cells from cytotoxic tBHP oxidative insult. Empty nanoparticles did not display any protective effect against oxidative damage, as compared to the control group (cells without tBHP) (Figure 11). Nevertheless, free and WSE-loaded nanoparticles significantly protected cells against tBHP-induced cytotoxicity (Figure 11 A, B and C). When compared with the free WSE, WSE-loaded MPEG-PCL nanoparticles demonstrated improved protective effect in all three tested concentrations. Among the nanoformulations, WSE-loaded MPEG-PCL nanoparticles offered higher cellular protection (42.2%) for 0.1 µg/mL, 88.8% for 1 µg/mL and 95.2% for 10 µg/mL. When compared, WSE-loaded PCL nanoparticles presented less protective effect (33.2%) for 0.1 µg/mL, 48.2% for 1 µg/mL, and 56.5% for 10 µg/mL.

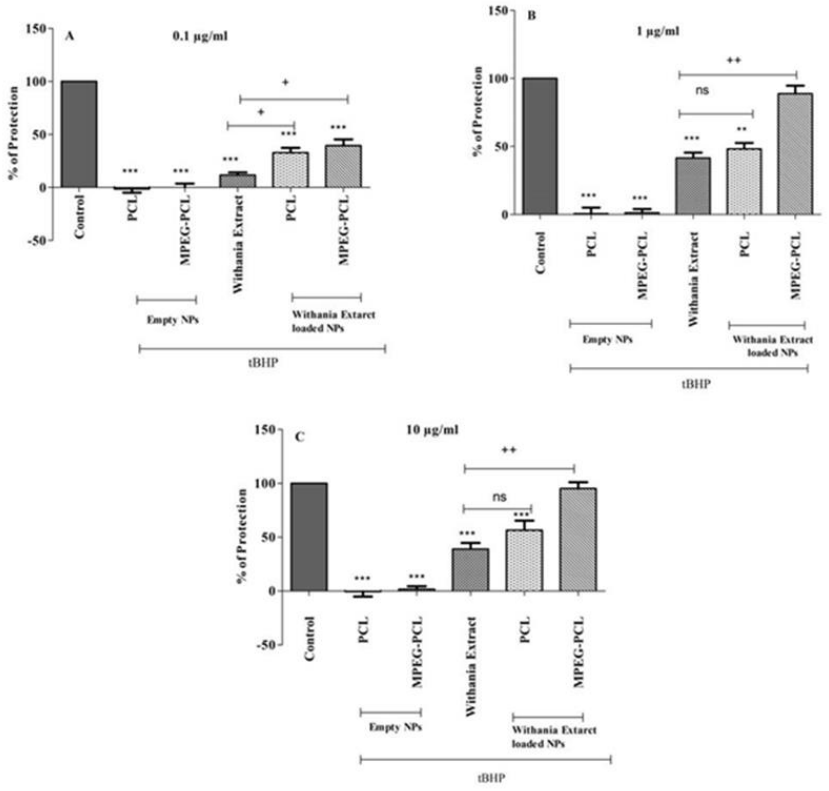

Figure 11 — Protection by WSE-loaded MPEG-PCL and PCL nanoparticles (NPs) at different concentrations (0.1, 1 and 10 µg/mL) against 1 mM tBHP-induced oxidative stress in U251 glioma cells. Data presented (mean±SD, n=3). Statistically significant differences from free WSE are annotated ($^{+}P<0.05$, $^{++}P<0.01$, $^{+++}P<0.001$, ns - not significant).

The levels of cell lipid peroxidation, evaluated by TBARS, increased significantly with tBHP insult (Figure 12). WSE and WSE-loaded nanoparticles, namely MPEG-PCL ones, reduced these levels significantly.

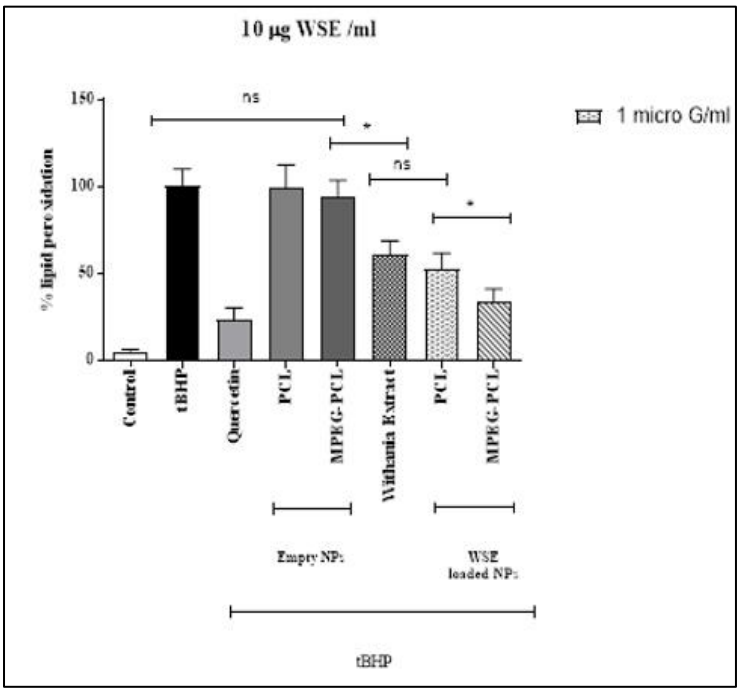

Figure 12 — Effect of free WSE (10µg/mL) and equivalent amounts of WSE-loaded in MPEG-PCL and in PCL nanoparticles (NPs) on lipid peroxidation levels induced by 1 mM tBHP (3 h) oxidative stress in U251 glioma cells. Control group corresponds to cells not submitted to tBHP insult (basal levels); quercetin (10 µM) was used as positive control for inhibition of lipid peroxidation; tBHP data correspond to full lipid peroxidation induction by oxidative insult. Data is presented as mean±SD of five independent experiments. All the values are significantly different from the control ones. Asterisks (*) denotes statistically significant different values signalized by segments (*P<0.05, ns -not significant).

3.9. *In vivo* biodistribution of nanoparticles in zebrafish embryos

To study the effect of using nanoparticles for WSE delivery, biodistribution was studied by image analysis on zebrafish embryos treated with the experimental control (water only) (**Figure 13 A, B**), empty PCL (**Figure 13 C**, **D**) and MPEG-PCL (**Figure 13 E**, **F**) nanoparticles did not permit to detect any fluorescence throughout development. On the contrary, those exposed to free WSE-C exhibited blurred green fluorescence (**Figure 13 G**, **H**). However, the fluorescence intensity observed on zebrafish embryos exposed to WSE-C-loaded PCL nanoparticles was relatively lower (**Figure 13 I**, **J**), than at those treated with WSE-C-loaded MPEG-PCL nanoparticles (**Figure 13 K**, **L**). It is important to highlight that both type of WSE-C-loaded nanoparticles were (in general) uniformly distributed within embryos.

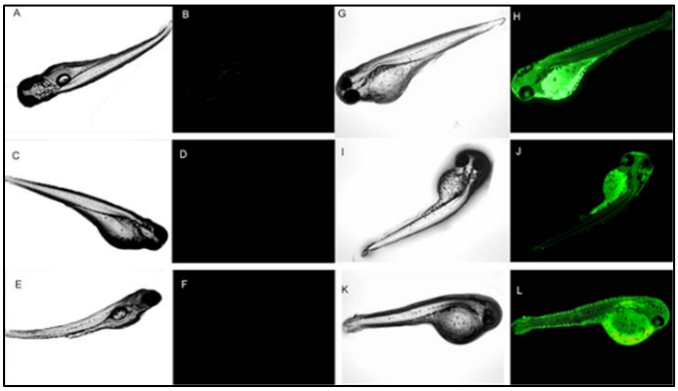

Figure 13 — Accumulation of WSE free and loaded at nanoparticles in 80 hpf zebrafish embryos. Microscopic photographic records were taken after 4 h incubation with free WSE-C and WSE-C-loaded nanoparticles. Light-fluorescent microscopic imaging of control zebrafish larvae (**A-B**). Light-fluorescent microscopic imaging of zebrafish larvae incubated with empty PCL nanoparticles (**C-D**). Light-fluorescent microscopic imaging of zebrafish larvae incubated with empty MPEG-PCL nanoparticles (**E-F**). Light-fluorescent microscopic imaging of zebrafish larvae incubated with free WSEC (**G-H**). Light-fluorescent microscopic imaging of zebrafish larvae incubated WSEC loaded PCL nanoparticles (**I-J**). Light-fluorescent microscopic imaging of zebrafish larvae incubated with WSEC loaded MPEG-PCL nanoparticles (**K-L**).

4. DISCUSSION

Poorly water-soluble drugs usually require high doses of oral administration in order to range therapeutic plasma levels. Low aqueous solubility is one of the most impacting hurdles for the development of novel therapeutic formulations, since under the aqueous cellular microenvironment, any drug to be efficiently absorbed at the target site should present high water solubility. However, a vast majority of the chemical entities used as drug agents are either weakly acidic or weakly basic having meagre aqueous solubility [25]. The excellent solubility shown by WSE encapsulated in PCL and in MPEG-PCL nanoparticles suggests that nanoencapsulation enhances aqueous solubility of the compounds. Among the nanoformulations, MPEG-PCL nanoparticles formed a clear solution in water, whereas PCL nanoparticles formed an emulsion indicating that the latter could be a better choice for WSE delivery.

Particle size is an important parameter, which can directly affect physical stability, cellular uptake, biodistribution and drug release from the nanoparticles. The difference perceived in the particle size

of empty and WSE encapsulated nanoparticles indicates that WSE has been incorporated into the polymer matrix. The superior size of the PCL nanoparticles compared to that of MPEG-PCL nanoparticles is probably due to the polymer's amphiphilic nature. Zeta potential is an indirect measurement of the surface charge, which in turn is important to determine the nanoparticles propensity to cluster in contact to blood proteins, or their tendency to adhere and/or interact with oppositely charged cell membranes [21, 26]. Both nanocarriers exhibited a negatively charged surface, with PCL nanoparticles demonstrating a higher degree, indicating potential stability under physiological conditions A successful nanocarrier system with high entrapment efficacy can diminish the amount of vehicle/load required for administration. The higher entrapment efficiency observed for MPEG-PCL nanoparticles combined with their morphological features, such as round morphology which favors interaction with cells, advocates for their successful use for therapy.

The DSC analysis revealed an amorphous or disordered crystalline nature of a molecular dispersion, or a solid solution state. XRD analysis further supported the amorphous state of WSE-loaded PCL and MPEG-PCL nanoparticles, while detecting a crystalline state for WSE in the polymer. Similar results were obtained before for curcumin-loaded PCL and MEPG-PCL nanoparticles [14].

Both PCL and MPEG-PCL nanoparticles loaded with WSE showed a controlled release pattern. A fast release, up to 30-40% in the first 6h, and then a slow release up to 80% at 162h. On the other hand in free WSE, up to 75% of the drug was released in the first 6h and circa 85% of the compounds were released within 24 h, highlighting that nanoformulations could be a good approach to achieve sustained release of these herbal extract drugs [27]. The molecular weight of the polymer, and the chain length of PEG and PCL groups, influenced the release of WSE from the nanoparticles. Higher content of MPEG generally leads to higher amounts of burst release of the drug, as PEG is hydrophilic in nature. Higher content of PCL groups leads to a continuous release of the drug, as PCL is lipophilic in nature [14]. In this work, the release of the drug was similar for both MPEG-PCL and PCL nanoparticles, although with higher levels for PCL loaded nanoparticles. This might be due the fact that the withanolides are in general lipophilic compounds that could have been more retained by MPEG nanoparticles. Oral drug administration does not regularly afford rate-controlled release, or target site specificity. Often, conventional drug delivery yields accentuated increases of drug concentration at potentially toxic levels. Here, we demonstrated that WSE was released in a sustained manner when delivered via nanoparticles (Fig. 7).

MTT assay is a well-established method for evaluating metabolic activity and redox status of animal cells, which are indicative of cell viability and may be extrapolated to indicate putative cytotoxicity of substances [28]. In this case, results were confirmed by LDH leakage assay by that loss of cell metabolic activity correlates with loss of cell viability (data not shown). Empty PCL and MPEG-PCL nanoparticles did not affect cell viability up to 500 μg/mL (data not shown), corroborating previously reported results [14]. WSE decreases cell viability in a concentration dependent manner, and specific concentrations of WSE-encapsulated PCL and MPEG-PCL nanoparticles not affecting cell viability could be selected.

Regarding cell uptake, compared to the free WSE-C, PCL and namely MPEG-PCL nanoparticles loaded with WSE-C were quickly uptaken by glioma cells. It is reasonable to speculate that this improved cell internalization is possibly due to better stability of the carriers containing PEG. Most probably, the cells have taken up particles via endocytosis, as similarly to other literature reports [29, 30].

Among the nanoformulations, WSE-loaded MPEG-PCL nanoparticles offered better protection for cells exposed to oxidative insult, even compared to WSE-loaded PCL nanoparticles. WSE and WSE-loaded nanoparticles, particularly MPEG-PCL, were effective in reducing lipid peroxidation, indicating that their cytoprotective effect is related with an antioxidant effect. Similar results were observed with PCL and MPEG-PCL nanoparticles filled with a neuroprotective extract of *Hypericum perforatum*, tested in HepG2 cells [31, 32].

The results here described demonstrated that free WSE could provide neuroprotection to U251 cells against oxidative stress induced by tBHP. Yet, this neuroprotective effect was less effective than that provided by WSE while encapsulated in the nanoparticles, at an equivalent nominal concentration. It was notably observed that WSE-loaded nanoparticles exhibited significant efficacy in protecting human glioma cells from oxidative insult, even at lower test concentrations. This capability can be attributed to their water solubility, enhanced cellular uptake, and controlled release of withanolides, resulting in an optimized concentration of these agents to effectively neutralize the production of free radicals in neuronal cells. These findings are in agreement with previous reports, not only regarding cell uptake capacity, but mostly on the neuroprotective effect provided by other drug-loaded nanoparticles in different neuronal cellular models. Other authors demonstrated that curcumin packing into poly (lactic-co-glycolic acid) (PLGA) nanoparticles augmented its neuroprotective effect against oxidative injury caused by Alzheimer's disease [33]. Other groups further substantiated PLGA nanoparticles neuroprotective competency by encapsulating nicotine, since the entrapment at these enhanced its bioavailability and thus, its subsequent capacity to modulate the oxidative stress and apoptosis indicators [34]. Also, sesamol-loaded solid lipid nanoparticle revealed to be a successful strategy to alleviate intracerebroventricular streptozotocin induced defected neuronal function and cognitive impairment [35].

Zebrafish embryogenesis is completed within 120 h_{pf}, representing a swift and proficient *in vivo* system to investigate vertebrate development. Higher fecundity rates permit the production of numerous externally-fertilized eggs that develop promptly into larvae within 5 days post-fertilization (d_{pf}) [36]. The developing embryos transparency makes possible to directly observe their internal organs and easily assess in real-time any agent/factor-induced alterations, posing thus reason to use these as imaging-model to fast-tracking the associated pathological processes. Moreover, being a teleost, its similarities to human embryonic development and the significant genetic homology are highly appreciated characteristics to detect early signs of developmental defects and modelling several pathologies in humans [37]. It has also been acknowledged as a robust model for large-scale

toxicology screenings [38]. Given the abovementioned advantages, 80 h_{pf}-aged zebrafish larvae were used to investigate *in vivo* biodistribution of the developed nanoparticles.
The obtained data seem to point to a higher efficient uptake of WSE-C once encapsulated in MPEG-PCL nanoparticles, which are known to have a greater potential for drug delivery, being already used successfully as vehicle of several drugs [39, 40]. MPEG-PCL nanoparticles' amphiphilicity, linear structure and uniform size might contribute as key factors [41]. Adding to this, it is well recognized that nanoparticles PEGylation tends to enhance blood circulation times and cell membrane entry pathways [42, 43].

5. CONCLUSION

Although phytomedicines based on WS possess excellent bioactivities, their low water solubility, greater molecular size, and general metabolic impact tend to limit their clinical outcome. Products derived from *Withania somnifera* have many different potential applications, and already an established relevant market share in nutraceuticals. Therefore, the improvement of their effectiveness is particularly appealing. In this study, WSE-loaded PCL and MPEG-PCL nanoparticles were developed to promote its aqueous solubility and cellular entry, and surmount damage mediated by oxidative agents. It was found that the protective effect of WSE against oxidative stress could be significantly improved by nanoencapsulation. As the polymers used in this study are non-toxic, biodegradable and biocompatible, apart from being FDA-approved, the nanoformulations developed in this work could be used as safe delivery nano-vehicles. Because of their small size and biodegradability, these can be administered parentally. *In vivo* localization analysis in zebrafish embryos revealed a favorable biodistribution of both PCL and MPEG-PCL nanoparticles, more concentrated in the nervous system. Together, obtained results allow to conclude that nanoencapsulation of WSE enhances the cellular uptake and protection against oxidative stress. Moreover, since WSE is widely used as a neuroprotective agent, its nanoparticles might be a way to increase its bioavailability and targeting to neurons. In future studies, these NPs could be used for delivery of other neuroprotective agents and further optimized for active targeting through surface modification with ligands, for full exploitation of their potential.

Acknowledgments. This work was supported by the "Contrato-Programa" UIDB/04050/2020 funded by national funds through the FCT I.P. https://doi.org/10.54499/UIDB/04050/2020, and FCT projects (PTDC/AGR-ALI/105169/2008 and PTDC/AGR-GPL/119211/2010). Gregory Marslin was supported by a FCT PhD fellowship (SFRH/BD/72809/2010). The authors acknowledge Mário Fernandes for assistance with the graphical abstract and Vanessa Pinho for the literature review.

Author Contributions. Conceptualization, AD, BS and AG; methodology, AD, OC, MP; validation, GM, MP, AD; formal analysis, GM; investigation, GM, JF and PM; resources, AD, AG; data curation, GM, MP; writing—original draft preparation, GM, MP, AD; writing—review and editing, AD, MP and AG; visualization, GM and MP; supervision, AD; project administration, AD and AG; funding acquisition, AD and AG. All authors have read and agreed to the published version of the manuscript.

Conflict of Interest. The authors declare no conflict of interest.

References

[1] T. A. Oyedepo and S. Palai, "Herbal remedies, toxicity, and regulations. reparation of phytopharmaceuticals for the management of disorders," in Academic Press, 2021, pp. 89-127. DOI: 10.1016/B978-0-12-820284-5.00014-9.

[2] A. G. Atanasov et al., "Natural products in drug discovery: advances and opportunities," *Nat Rev Drug Discov*, vol. 20, pp. 200–216, 2021. DOI: 10.1038/s41573-020-00114-z.

[3] S. Paul et al., "*Withania somnifera* (L.) Dunal (Ashwagandha): A comprehensive review on ethnopharmacology, pharmacotherapeutics, biomedicinal and toxicological aspects," *Biomedicine & Pharmacotherapy*, vol. 143, p. 112175, 2021. DOI: 10.1016/j.biopha.2021.112175.

[4] T. K. Smith et al., "Herbal supplement sales in US increase by record-breaking 17.3% in 2020" *HerbalGram*, vol. 131, pp. 52-65, 2021.

[5] A. L. Lopresti and S. J. Smith, "Ashwagandha (*Withania somnifera*) for the treatment and enhancement of mental and physical conditions: A systematic review of human trials," *Journal of Herbal Medicine*, vol. 28, p. 100434, 2021. DOI: 10.1016/j.hermed.2021.100434.

[6] N. Alam et al., "High catechin concentrations detected in Withania somnifera (Ashwagandha) by high performance liquid chromatography analysis," *BMC Complement Altern. Med*., vol. 11, 2011, Art. no. 65. DOI: 10.1186/1472-6882-11-65.

[7] V. Pandey et al., "Withania somnifera: Advances and implementation of molecular and tissue culture techniques to enhance its application," *Front. Plant Sci*., vol. 8, 2017, Art. no. 1390. DOI: 10.3389/fpls.2017.01390.

[8] S. Paroha et al., "Conventional and nanomaterial-based techniques to increase the bioavailability of therapeutic natural products: a review," *Environ Chem Lett*, vol. 18, pp. 1767–1778, 2020. DOI: 10.1007/s10311-020-01038-1.

[9] C. Hu et al., "Micelle or polymersome formation by PCL-PEG-PCL copolymers as drug delivery systems," *Chinese Chemical Letters*, vol. 28, no. 9, pp. 1905-1909, 2017. DOI: 10.1016/j.cclet.2017.07.020.

[10] R. Saka and N. Chella, "Nanotechnology for delivery of natural therapeutic substances: a review," *Environ Chem Lett,* vol. 19, pp. 1097–1106, 2021. DOI: 10.1007/s10311-020-01103-9.

[11] N. P. Aditya et al., "Fabrication of amorphous curcumin nanosuspensions using beta-lactoglobulin to enhance solubility, stability, and bioavailability," *Colloids Surf. B Biointerfaces*, vol. 127, pp. 114-121, 2015. DOI: 10.1016/j.colsurfb.2015.01.027.

[12] B. Ray et al., "Neuroprotective and neurorescue effects of a novel polymeric nanoparticle formulation of curcumin (NanoCurc) in the neuronal cell culture and

animal model: implications for Alzheimer's disease," *J. Alzheimers Dis*., vol. 23, pp. 61-77, 2011. DOI: 10.3233/JAD-2010-101374.

[13] S. Dhawan et al., "Formulation development and systematic optimization of solid lipid nanoparticles of quercetin for improved brain delivery," *J. Pharm. Pharmacol.*, vol. 63, pp. 342-351, 2011. DOI: 10.1111/j.2042-7158.2010.01225.x.

[14] G. Marslin et al., "Curcumin encapsulated into methoxy poly(ethylene glycol) poly(epsilon-caprolactone) nanoparticles increases cellular uptake and neuroprotective effect in glioma cells," *Planta Med*., vol. 83, pp. 434-444, 2017. DOI: 10.1055/s-0042-112030.

[15] D. M. Teleanu et al., "Blood-Brain Delivery Methods Using Nanotechnology," *Pharmaceutics*, vol. 10, no. 4, p. 269, Dec. 2018. DOI: 10.3390/pharmaceutics10040269.

[16] J. Ribeiro et al., "A New Perspective for the Treatment of Alzheimer's Disease: Exosome-like Liposomes to Deliver Natural Compounds and RNA Therapies," *Molecules*, vol. 28, no. 16, p. 6015, 2023. DOI: 10.3390/molecules28166015.

[17] M. N. Ragnaill et al., "Internal benchmarking of a human blood-brain barrier cell model for screening of nanoparticle uptake and transcytosis," *Eur. J. Pharm. Biopharm*., vol. 77, pp. 360-367, 2011. DOI: 10.1016/j.ejpb.2010.12.024.

[18] H. Danafar and U. Schumacher, "MPEG–PCL copolymeric nanoparticles in drug delivery systems," *Cogent Medicine*, vol. 3, 2016, Art. no. 1142411. DOI: 10.1080/2331205X.2016.1142411.

[19] OECD, "Test No. 203: Fish, Acute Toxicity Test," in *OECD Guidelines for the Testing of Chemicals*, Section 2, OECD Publishing, Paris, 2019. DOI: 10.1787/9789264070144-en.

[20] A. C. N. Oliveira et al., "Counter ions and constituents combination affect DODAX:MO nanocarriers toxicity in vitro and in vivo," *Toxicol. Res*. (Camb.), vol. 5, pp. 1244-1255, 2016. DOI: 10.1039/C6TX00074F.

[21] H. Danafar et al., "Biodegradable m-PEG/PCL core-shell micelles: preparation and characterization as a sustained release formulation for curcumin," *Adv. Pharm. Bull*., vol. 4, pp. 501-510, 2014. DOI: 10.5681/apb.2014.074.

[22] H. Gao et al., "Ligand modified nanoparticles increases cell uptake, alters endocytosis and elevates glioma distribution and internalization," *Sci. Rep*., vol. 3, 2013, Art. no. 2534. DOI: 10.1038/srep02534.

[23] P. Dumont et al., "Overexpression of apolipoprotein J in human fibroblasts protects against cytotoxicity and premature senescence induced by ethanol and tert-butylhydroperoxide," *Cell Stress Chaperones*, vol. 7, pp. 23-35, 2002. DOI: 10.1379/1466-1268(2002)007<0023:ooajih>2.0.co;2.

[24] Y. J. Shin et al., "Protective effect of clusterin on oxidative stress-induced cell death of human corneal endothelial cells," *Mol. Vis*., vol. 15, pp. 2789-2795, 2009. PMID: 20019877; PMCID: PMC2793897.

[25] K. T. Savjani et al., "Drug solubility: importance and enhancement techniques," *ISRN Pharm*., 2012, Art. no. 195727. DOI: 10.10.5402/2012/195727.

[26] A. Kumari et al., "Biodegradable polymeric nanoparticles based drug delivery systems," *Colloids Surf. B Biointerfaces*, vol. 75, pp. 1-18, 2010. DOI: 10.1016/j.colsurfb.2009.09.001.

[27] V. Karanam et al., "Poly (varepsilon-caprolactone) nanoparticles of carboplatin: Preparation, characterization and in vitro cytotoxicity evaluation in U-87 MG cell lines," *Colloids Surf. B Biointerfaces*, vol. 130, pp. 48-52, 2015. DOI: 10.1016/j.colsurfb.2015.04.005.

[28] P. W. Sylvester, "Optimization of the tetrazolium dye (MTT) colorimetric assay for cellular growth and viability," in *Methods Mol. Biol*, 2011, vol. 716, pp. 157-168. DOI: 10.1007/978-1-61779-012-6_9.

[29] R. T. Carroll et al., "Brain-targeted delivery of Tempol-loaded nanoparticles for neurological disorders," *J. Drug Target*, vol. 18, pp. 665-674, 2010. DOI: 10.3109/10611861003639796.

[30] D. Ding et al., "Cisplatin-loaded gelatin-poly(acrylic acid) nanoparticles: synthesis, antitumor efficiency in vivo and penetration in tumors," *Eur. J. Pharm. Biopharm*., vol. 79, pp. 142-149, 2011. DOI: 10.1016/j.ejpb.2011.01.008.

[31] A. C. Carvalho et al., "Methanolic extract of *Hypericum perforatum* cells elicited with Agrobacterium tumefaciens provides protection against oxidative stress induced in human HepG2 cells," *Ind. Crops Prod*., vol. 59, pp. 177-183, 2014. DOI: 10.1016/j.indcrop.2014.05.018.

[32] A. Oliveira et al., "Development, characterization, antioxidant and hepatoprotective properties of poly(Ɛ-caprolactone) nanoparticles loaded with a neuroprotective

fraction of Hypericum perforatum," *International Journal of Biological Macromolecules*, vol. 110, pp. 185-196, 2018. DOI: 10.1016/j.ijbiomac.2017.10.103.

[33] S. Doggui et al., "Neuroprotective efficacy of curcumin-loaded nanoparticles in Parkinson's disease model of zebrafish," *Mol. Neurodegener.*, vol. 6, 2011, Art. no. 28. DOI: 10.1186/1750-1326-6-28.

[34] M. N. Tiwari et al., "Nicotine-encapsulated poly(lactic-co-glycolic) acid nanoparticles improve neuroprotective efficacy against MPTP-induced parkinsonism," *Free Radic. Biol. Med.*, vol. 65, pp. 704-718, 2013. DOI: 10.1016/j.freeradbiomed.2013.07.042.

[35] A. K. Sachdeva et al., "Neuroprotective potential of sesamol and its loaded solid lipid nanoparticles in ICV-STZ-induced cognitive deficits: behavioral and biochemical evidence," *Eur. J. Pharmacol.*, vol. 747, pp. 132-140, 2015. DOI: 10.1016/j.ejphar.2014.11.014.

[36] C. B. Kimmel et al., "Stages of embryonic development of the zebrafish," *Dev. Dyn.*, vol. 203, pp. 253-310, 1995. DOI: 10.1002/aja.1002030302.

[37] G. Kari et al., "Zebrafish: an emerging model system for human disease and drug discovery," *Clin. Pharmacol. Ther.*, vol. 82, pp. 70-80, 2007. DOI: 10.1038/sj.clpt.6100223.

[38] N. S. Sipes et al., "Zebrafish: as an integrative model for twenty-first century toxicity testing," *Birth Defects Res. C Embryo Today*, vol. 93, pp. 256-267, 2011. DOI: 10.1002/bdrc.20214.

[39] W. Peng et al., "Oral delivery of capsaicin using MPEG-PCL nanoparticles," *Acta Pharmacol. Sin*., vol. 36, pp. 139-148, 2015. DOI: 10.1038/aps.2014.113.

[40] K. Wang et al., "Preparation and in vitro release of buccal tablets of naringenin-loaded MPEG-PCL nanoparticles," *RSC Advances*, vol. 4, pp. 33672-33679, 2014. DOI: 10.1039/C4ra04920a.

[41] T. W. Shen et al., "Distribution and cellular uptake of pegylated polymeric particles in the lung towards cell-specific targeted delivery," *Pharm. Res*., vol. 32, pp. 3248–3260, 2015. DOI: 10.1007/s11095-015-1701-7.

[42] J. V. Jokerst et al., "Nanoparticle PEGylation for imaging and therapy," *Nanomedicine*, vol. 6, pp. 715-728, 2011. DOI: 10.2217/Nnm.11.19.

[43] N. Vij et al., "Development of PEGylated PLGA nanoparticle for controlled and sustained drug delivery in cystic fibrosis," J. *Nanobiotechnology*, vol. 8, 2010, Art. no. 22. DOI: 10.1186/1477-3155-8-22.

*[a] CENTRE FOR THE RESEARCH AND TECHNOLOGY OF AGRO-ENVIRONMENT AND BIOLOGICAL SCIENCES (CITAB-UM), AGROBIOPLANT GROUP, DEPARTMENT OF BIOLOGY, UNIVERSITY OF MINHO, BRAGA, PORTUGAL
[b] CESPU - INSTITUTO DE INVESTIGAÇÃO E FORMAÇÃO AVANÇADA EM CIÊNCIAS E TECNOLOGIAS DA SAÚDE, RUA CENTRAL DE GANDRA 1317, 4585-116 GANDRA, PORTUGAL
[c] INEB - INSTITUTO NACIONAL DE ENGENHARIA BIOMÉDICA, UNIVERSIDADE DO PORTO, RUA ALFREDO ALLEN 208, 4200-393 PORTO, PORTUGAL
[d] I3S - INSTITUTO DE INVESTIGAÇÃO E INOVAÇÃO EM SAÚDE, UNIVERSIDADE DO PORTO, RUA ALFREDO ALLEN 208, 4200-393 PORTO, PORTUGAL
[e] CENTRO DE BIOLOGIA MOLECULAR E AMBIENTAL (CBMA), DEPARTMENT OF BIOLOGY, UNIVERSITY OF MINHO, BRAGA, PORTUGAL
[f] INL - INTERNATIONAL IBERIAN NANOTECHNOLOGY LABORATORY, BRAGA, PORTUGAL

Correspondence: agomes@bio.uminho.pt (ACG); albertocpdias66@gmail.com (ACPD)